



Finite element model for linear-elastic mixed mode loading using adaptive mesh strategy

Miloud SOUIYAH[†], Abdunaser ALSHOAIBI, A. MUCHTAR, A.K. ARIFFIN

(Department of Mechanical & Materials Engineering, Universiti Kebangsaan Malaysia, Bangi, Selangor 43600, Malaysia)

[†]E-mail: miloud20@eng.ukm.my

Received Aug. 1, 2007; revision accepted Oct. 16, 2007; published online Dec. 8, 2007

Abstract: An adaptive mesh finite element model has been developed to predict the crack propagation direction as well as to calculate the stress intensity factors (SIFs), under linear-elastic assumption for mixed mode loading application. The finite element mesh is generated using the advancing front method. In order to suit the requirements of the fracture analysis, the generation of the background mesh and the construction of singular elements have been added to the developed program. The adaptive remeshing process is carried out based on the posteriori stress error norm scheme to obtain an optimal mesh. Previous works of the authors have proposed techniques for adaptive mesh generation of 2D cracked models. Facilitated by the singular elements, the displacement extrapolation technique is employed to calculate the SIF. The fracture is modeled by the splitting node approach and the trajectory follows the successive linear extensions of each crack increment. The SIFs values for two different case studies were estimated and validated by direct comparisons with other researchers work.

Key words: Linear-elastic fracture mechanics, Adaptive refinement, Stress intensity factors (SIFs), Crack propagation

doi:10.1631/jzus.A072176

Document code: A

CLC number: O39

INTRODUCTION

The use of crack propagation laws based on stress intensity factor (SIF) is the most successful engineering application of fracture mechanics. This characterizes the SIFs as of the most important parameters in fracture analysis. In the elastic fracture analysis, the SIFs sufficiently define the stress field close to the crack tip and provide fundamental information on how the crack is going to propagate. Basically, the estimation methods can be categorized into two groups, those based on field extrapolation near the crack tip and those which use the energy release when the crack propagates. The latter group includes J -contour integration, the virtual crack extension and the strain energy release rate method. The main disadvantage of these methods is that the SIF components, K_I and K_{II} in mixed mode application are either impossible or very difficult to be separated. Nevertheless, the first group which is based on near-tip field fitting procedures requires finer meshes

to produce a good numerical representation of crack-tip fields. Usually, the singular point elements are generated to facilitate the calculation (de Araújo *et al.*, 2000).

One of the simplest and most frequently used methods is displacement extrapolation. It functions typically in obtaining displacement jumps along the crack faces and then applying the elasticity relations to compute a set of estimated SIF values (de Murais, 2007). In order to predict the fracture direction and loading based on the concept of Maximum Potential Energy Release Rate (MPERR), a new general mixed-mode brittle fracture criterion was applied by Chang *et al.* (2006). The calculation and comparison of the SIFs have been obtained for a cracked Element Free Galerkin Method (EFGM) plate by using several different numerical techniques (Anlas *et al.*, 2000).

A study of subcritical crack growth in Zirconia-toughened alumina (ZTA) ceramics was carried out by Szutkowska and Boniecki (2006). The crack length was evaluated by linear-elastic analysis from

the compliance of single-edge-notched specimen in three-points bending test. The finite element method has been proven to be very well suited for the study of fracture mechanics. Nevertheless the modeling of crack propagation through a finite element mesh turned out to be difficult because of the modification of the mesh topology. Nodal relaxation is frequently used to release nodes, in order to enable the crack tip to propagate through the mesh (Phongthanapanich and Dechaumphai, 2004).

The paper aims to determine the SIFs for crack propagation problem under linear-elastic fracture analysis by means of a displacement extrapolation technique with adaptive mesh finite element method. The source code of the program on this study is written in FORTRAN 98. The mesh for finite elements is the unstructured type, generated using the advancing front method. The global h -type adaptive mesh is adopted based on the norm stress error estimator. The quarter-point singular elements are uniformly generated around the crack tip in the form of a rosette. The displacement extrapolation technique used in the calculation is explained. Two different test specimens' geometries were considered, i.e. three points bending specimen and the central cracked plate.

SIF AND CRACK PROPAGATION

In this paper, the displacement extrapolation method (Guinea et al., 2000) is used to calculate the SIFs as follows:

$$K_I = \frac{E}{3(1+\nu)(1+\kappa)} \sqrt{\frac{2\pi}{L}} \left[4(v'_b - v'_d) - \frac{(v'_c - v'_e)}{2} \right], \quad (1)$$

$$K_{II} = \frac{E}{3(1+\nu)(1+\kappa)} \sqrt{\frac{2\pi}{L}} \left[4(u'_b - u'_d) - \frac{(u'_c - u'_e)}{2} \right], \quad (2)$$

where E is the modulus of elasticity; ν is Poisson's ratio; κ is the elastic parameter; L is the quarter-point element length; u' and v' are the displacement components in the x' and y' directions, respectively; the subscripts indicate their positions as shown in Fig.1.

$$\kappa = \begin{cases} (3-4\nu), & \text{plane stress;} \\ (3-4\nu)/(1+\nu), & \text{plane strain.} \end{cases} \quad (3)$$

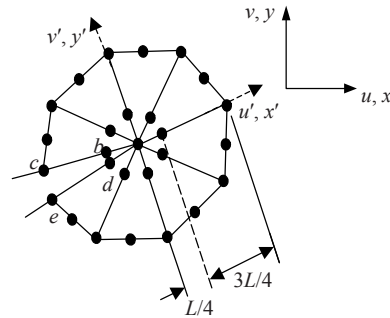


Fig.1 Crack face coordinate frame versus global coordinate frame

MESH GENERATION AND ADAPTIVE REFINEMENT

In this work, the unstructured triangular mesh is automatically generated by employing the advancing front method (Löhner, 1997). The latest review of this method can be found in the previous research (Zienkiewicz et al., 2005). In order to represent the field singularity correctly at the crack tip, the singular elements have to be constructed. In our implementation, these special elements as shown in Fig.1 are generated separately from the conventional ones using a cut and paste procedure. An impressive discussion on the adaptive mesh generators is given in (Alshoaibi et al., 2007).

In general, smaller mesh size gives more accurate finite element approximate solution. However, a reduction in the mesh size leads to greater computational effort. The adaptive mesh refinement is employed as the optimization scheme. This scheme is based on a posteriori error estimator obtained from the solution of the previous mesh. Here stress error norm is taken as the error estimator. The strategy used to refine the mesh during the analysis process is adopted from (Alshoaibi and Ariffin, 2006).

In order to properly represent the field singularity around the crack tip, the singular elements have to be constructed as well. Since the advancing front method generates the triangle elements starting from the boundary faces, the area around the crack tip for the construction of the singular elements is supposed to be isolated. This area is isolated by firstly generating nodes around the crack tip in the rosette form. After that, the crack tip node and the jointed boundary segments are removed. New boundary segments are

then introduced linking all the new nodes to temporarily 'cut out' the template area from the original domain. Subsequently the advancing front triangulation can be executed. Finally singular elements are 'patched' into the rosette template to complete the process. This procedure in Fig.2 is quite similar to that from a previous work (de Matos *et al.*, 2004). The number of elements depends on the distributed nodes around the crack tip, which can be set by the user. Here the natural triangular quarter point elements (Freese and Tracey, 1976) are used instead of the collapse quadrilateral element (Barsoum, 1976).

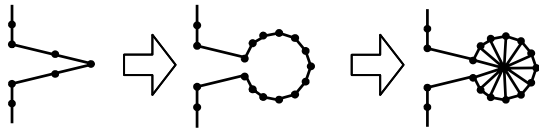


Fig.2 The cut and patch procedure of generating singular elements around a crack tip

NUMERICAL ANALYSIS AND VALIDATION

In order to carry out a comprehensive evaluation of the SIFs approximated by the developed program, two well-known plate geometries are used: single edge cracked plate with three holes and with four points bending.

Single edge cracked plate with three holes under mixed mode loading

A fracture problem under a complicated mixed mode has been studied, to demonstrate the performance of the developed program to model the crack propagation from initial notches in a single edge cracked plate with three holes and accurately predict the values of SIFs. The geometry of the single edge cracked plate with three holes and its final adaptive mesh are shown in Figs.3 and 4.

The material is polymethylmethacrylate (PMMA beam), which has Young's modulus of $E=210$ GPa and Poisson's ratio of $\nu=0.3$. It is clear that PMMA is considered as brittle material; however, the results obtained are applicable to any kind of material as long as LEFM is valid. The plate is simply supported near the lower corners, and subjected to a concentrated load at the center of the upper edge.

The experiments conducted by Bittencourt *et al.*

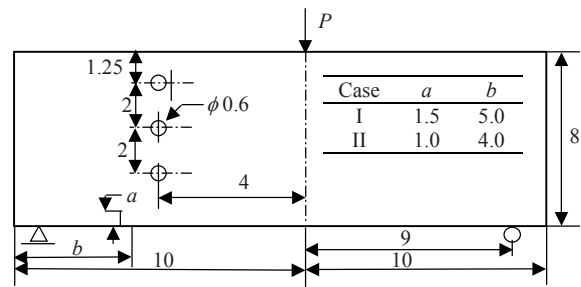


Fig.3 The geometry of the single edge cracked plate with three holes

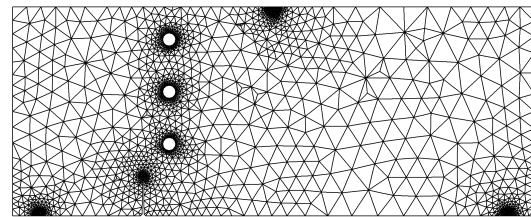


Fig.4 The final adaptive mesh of the single edge crack plate with three holes

(1996) are used as benchmark to validate the results of the present study with two cases of the initial crack length, a , and its location, b , as shown by the table in Fig.3. This configuration was chosen because two different crack growth trajectories had been predicted by the finite element modeling of the holed specimens, depending on the initial notch geometry.

For case I, the initial crack length, a , and its location, b , are 1.5 and 5.0 units, respectively. The results of the adaptive finite element meshes and the crack growth trajectory are depicted in Fig.5a. The figure shows that the crack growth trajectory passes just above the lower hole and ends at the middle hole.

As expected, there was significant difference in crack trajectories between Figs.5 and 6. The results proved that the crack trajectory was dependent on the initial crack location. An initial location close to the hole could cause the crack path to go towards the hole, while the crack path far from initial locations remotes from the hole. As can be seen in Fig.6, the crack trajectory still moved towards the hole although the initial crack was far from the hole compared to that in Fig.5.

For case II, the results of the present study for the crack path prediction is also compared qualitatively with the numerical results using enriched element free Galerkin method (EFGM) (Ventura *et al.*, 2001) and the extended finite element method results (X-FEM)

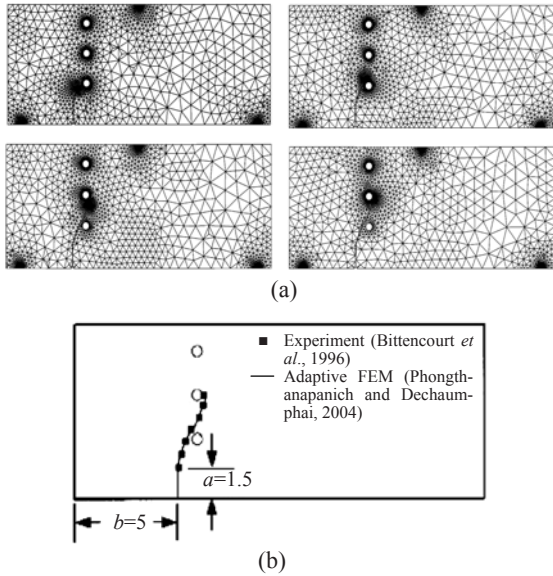


Fig.5 (a) Present results on adaptive finite element meshes and the crack growth trajectory for the single edge cracked plate with three holes; (b) Experimental and FEM trajectory (case I)

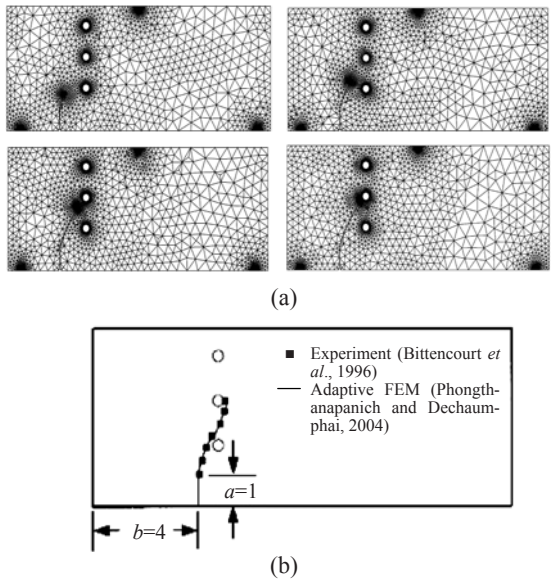


Fig.6 (a) Present results on adaptive finite element meshes and the crack growth trajectory for the single edge cracked plate with three holes; (b) Experimental and FEM trajectory (case II)

(Bordas and Moran, 2006) as shown in Figs.7a and 7b respectively with good agreement.

The predicted values of the SIFs for mode I and mode II during crack propagation steps are compared with those results observed by Bittencourt *et al.*(1996), for the same geometry and boundary con-

ditions as shown in Fig.8. There seems to be good agreement for SIFs values in both modes for case I. However, the values of SIFs differed somewhat when the crack was in the neighborhood of a hole represented in Fig.8 by the sharp notches of decreasing SIFs.

Fig.9 shows the maximum principal stress distribution for the final step of the crack propagation for both cases.

The results in Fig.9 showed a slightly different stress distribution for each specimen. Note that, for

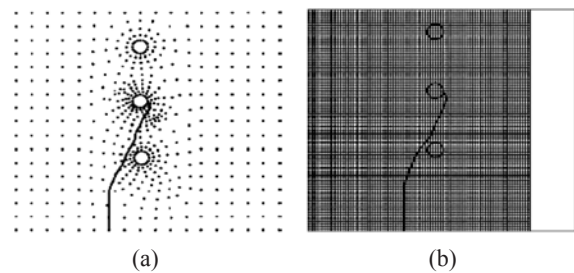


Fig.7 Crack propagation path for case II. (a) EFGM (Bittencourt *et al.*, 1996); (b) X-FEM (Ventura *et al.*, 2001)

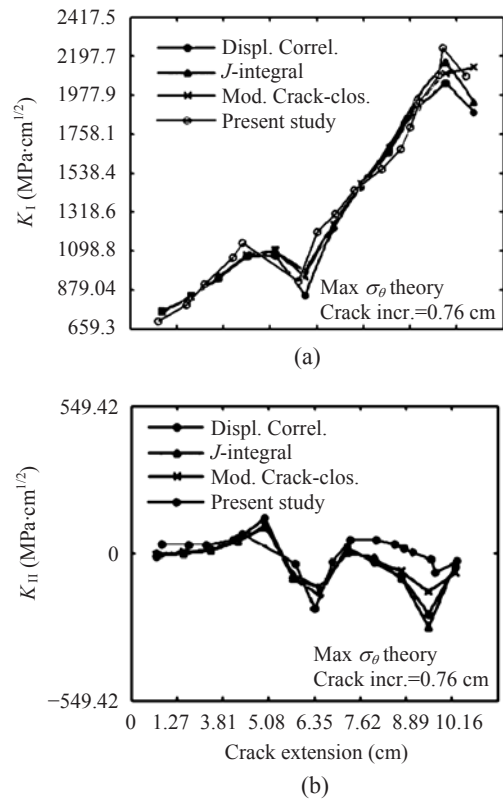


Fig.8 Comparison of SIF histories for case I between present results and those of Bittencourt *et al.*(1996) (a) Mode I; (b) Mode II

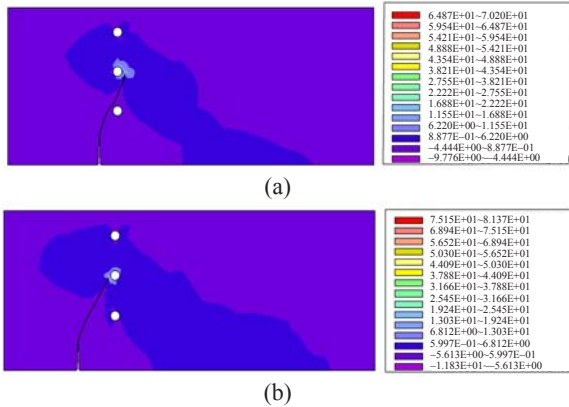


Fig.9 Maximum principal stress distribution for the single edge cracked plate with three holes. (a) Case I; (b) Case II

case I, the stress on the left-hand side was less than that on the right-hand side. For case II, the stress on the left-hand side was higher than that on the right-hand side. As a consequence, the crack propagated inwards starting from the boundary, towards the region where the stresses were much higher.

Four points bending specimen

A finite element model of linear-elastic fracture has been employed on four points bending specimen under mixed mode conditions with point loading applied, having thickness $B=3.5$ mm, height $W=4.5$ mm and length $L>43$ mm, made of Al_2O_3 -ceramics. The geometry of four points bending specimen and its final adaptive mesh, and the enlargement of mesh around the crack tip are shown in Figs.10 and 11.

The stresses in this loading case were also computed. The geometric functions F_I and F_{II} are defined as (Filon, 1903):

$$K_I = \frac{P}{WB} \left(1 - \frac{d}{L}\right) \sqrt{\pi a F_I}, \quad K_{II} = \frac{P}{WB} \left(1 - \frac{d}{L}\right) \sqrt{\pi a F_{II}}. \quad (4)$$

The geometry is imposed by plane strain condition with point load P , length L , height W , thickness B and crack length a . Somehow with this loading applied (i.e. point load) on four point bending specimen, it seems that the crack propagated straight forward as illustrated in Fig.12. The dimensionless SIF for this specimen is given in (Fett et al., 1995).

A comparison for the SIFs (K_I and K_{II}) values between the current results with those of Fett et al.(1995) are shown in Tables 1 and 2 with $d/W=0.5$.

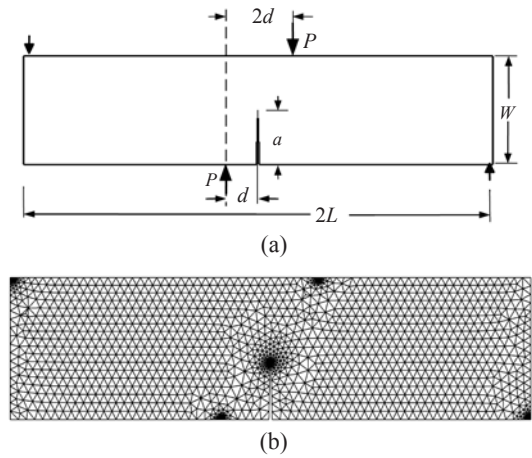


Fig.10 The geometry of the four points bend specimen (a) and its final adaptive mesh (b)

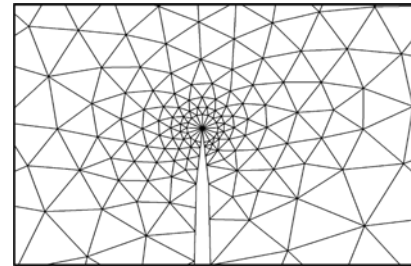


Fig.11 Enlargement of mesh around crack tip to represent the rosette elements

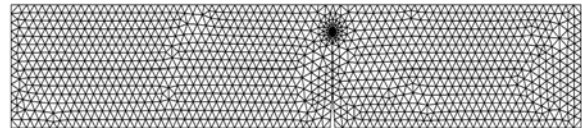


Fig.12 Crack propagation direction for the four points bend specimen

The dimensionless form of the estimated SIF is obtained by Eq.(4). Presented for a range of $0.1 < a/W < 0.4$. The results in the present study seem to be very close to those of Fett et al.(1995).

Table 1 Dimensionless SIF for central crack plate for mode I in case II

a/W	Fett et al.(1995)	Present study
0.1	0.3450	0.3461
0.2	0.6633	0.6660
0.3	0.9399	0.9354
0.4	1.1702	1.1721
0.6	1.5507	1.5512
0.8	2.0684	2.0697

Table 2 Dimensionless SIF for central crack plate for mode II in case II

a/W	Fett et al.(1995)	Present study
0.1	0.3841	0.3860
0.2	0.2448	0.2480
0.3	0.1580	0.1583
0.4	0.1098	0.1079
0.6	0.0566	0.0570
0.8	0.0106	0.0130

CONCLUSION

In this paper, a comprehensive finite element model was developed with an advancing front method for crack propagation analysis. The prediction of SIFs was as well considered under mixed mode loading, using an adaptive mesh strategy. The norm stress error is taken as a posterior estimator for the h -type adaptive refinement. The nodes of natural six-node quarter point elements generated around the crack tip were employed to form a circular zone surrounding the tip in order to capture better stress field. The adaptive remeshing technique places small elements around the crack tips and in region with large change of stress gradients. Larger elements are generated in other regions to minimize the total number of unknowns and the computational time. The accuracy of the estimated SIFs has been evaluated through assessments comprising two standard specimens. The results of SIFs are compared to the closed form solutions and to the extensive results of other studies. The crack simulations for modes I and II show acceptable crack path predictions. The obtained findings from the applied simulations strongly indicated that the numerical finite element solution has been successfully employed for 2D linear-elastic fracture mechanics problems.

References

- Alshoabi, A.M., Ariffin, A.K., 2006. Finite element simulation of stress intensity factors in elastic-plastic crack growth. *J. Zhejiang Univ. Sci. A*, **7**(8):1336-1342. [doi:10.1631/jzus.2006.A1336]
- Alshoabi, A.M., Hadi, M.S.A., Ariffin, A.K., 2007. An adaptive finite element procedure for crack propagation analysis. *J. Zhejiang Univ. Sci. A*, **8**(2):228-236. [doi:10.1631/jzus.2007.A0228]
- Anlas, G., Santare, M., Lambros, J., 2000. Numerical calculation of stress intensity factors in functionally graded materials. *Int. J. Fracture*, **104**(2):131-143. [doi:10.1023/A:1007652711735]
- Barsoum, R.S., 1976. On the use of isoparametric finite element in linear fracture mechanics. *International Journal of Numerical Methods in Engineering*, **10**(1):25-37. [doi:10.1002/nme.1620100103]
- Bittencourt, T.N., Wawrzynek, P.A., Ingraffea, A.R., Sousa, J.L.A., 1996. Quasi-automatic simulation of crack propagation for 2D LEFM problems. *Engineering Fracture Mechanics*, **55**(2):321-334. [doi:10.1016/0013-7944(95)00247-2]
- Bordas, S., Moran, B., 2006. Enriched finite elements and level sets for damage tolerance assessment of complex structures. *Engineering Fracture Mechanics*, **73**(9):1176-1201. [doi:10.1016/j.engfracmech.2006.01.006]
- Chang, J., Quan, X.J., Mutoh, Y., 2006. A general mixed-mode brittle fracture criterion for cracked materials. *Engineering Fracture Mechanics*, **73**(9):1249-1263. [doi:10.1016/j.engfracmech.2005.12.011]
- de Araujo, T., Bittencourt, T., Roehl, D., Martha, L., 2000. Numerical Estimation of Fracture Parameters in Elastic and Elastic-plastic Analysis. European Congress on Computational Methods in Applied Sciences and Engineering, Barcelona.
- de Matos, P.F.P., Moreira, P.M., Portela, A., de Castro, P.M., 2004. Dual boundary element analysis of cracked plates: post-processing implementation of the singularity subtraction technique. *Computers and Structures*, **82**(17-19):1443-1449. [doi:10.1016/j.compstruc.2004.03.040]
- de Murais, A.B., 2007. Calculation of stress intensity factors by the force method. *Engineering Fracture Mechanics*, **74**(5):739-750. [doi:10.1016/j.engfracmech.2006.06.017]
- Fett, T., Gerteisen, G., Hahnenberger, S., Martin, G., Munz, D., 1995. Fracture tests for ceramics under mode-I, mode-II and mixed-mode loading. *Journal of the European Ceramic Society*, **15**(4):307-312. [doi:10.1016/0955-2219(95)90353-K]
- Filon, L., 1903. On an approximate solution for the bending of a beam of rectangular cross-section under any system load, with special reference to points of concentrated or discontinuous loading. *Philosophical Transactions of the Royal Society of London, Series A*, **201**(1):63-155. [doi:10.1098/rsta.1903.0014]
- Freese, C.E., Tracey, D.M., 1976. The natural triangle versus collapsed quadrilateral for elastic crack analysis. *Int. J. Fracture*, **12**:767-770.
- Guinea, G.V., Planas, J., Elices, M., 2000. K_I evaluation by the displacement extrapolation technique. *Engineering Fracture Mechanics*, **66**(3):243-255. [doi:10.1016/S0013-7944(00)00016-3]
- Löhner, R., 1997. Automatic unstructured grid generators. *Finite Elements in Analysis and Design*, **25**(1-2):111-134. [doi:10.1016/S0168-874X(96)00038-8]
- Phongthanapanich, S., Dechaumphai, P., 2004. Adaptive Delaunay triangulation with object-oriented programming for crack propagation analysis. *Finite Elements in Analysis and Design*, **40**(13-14):1753-1771. [doi:10.1016/j.fin.2004.01.002]
- Szutkowska, M., Boniecki, M., 2006. Subcritical crack growth in Zirconia-toughened alumina (ZTA) ceramics. *Journal of Materials Processing Technology*, **175**(1-3):416-420. [doi:10.1016/j.jmatprotec.2005.04.030]
- Ventura, G., Xu, J.X., Belytschko, T., 2001. Level Set Crack Propagation Modelling in the Element-free Galerkin Method. Int. European Conference on Computational Mechanics.
- Zienkiewicz, O., Taylor, R., Zhu, J., 2005. The Finite Element Method: Its Basis and Fundamentals. Baker & Taylor Books.